Graphene Oxide as An Efficient Photocatalyst For Photocatalytic Reduction of CO_2 Into Solar Fuel

N. Shehzad[1, 3], K. Johari[1*], T. Murugesan[1] and M. Tahir[2,3]

[1]Department of Chemical Engineering, Faculty of Engineering,
Universiti Teknologi PETRONAS, 32610, Bandar Seri Iskandar, Perak, Malaysia
*Email: khairiraihana.j@utp.edu.my,
Tel: +605-3687684, Fax: +605–3686176
[2]Chemical Reaction Engineering Group (CREG),
Faculty of Chemical and Energy Engineering, Universiti Teknologi Malaysia,
81310 UTM, Skudai, Johor Bahru, Johor, Malaysia
[3]Department of Chemical Engineering, COMSATS Institute of Information
Technology, Defence Road, Off Raiwind Road, Lahore 54000, Pakistan

ABSTRACT

Photocatalytic reduction of CO_2 into solar fuel such as methane and methanol, is an attractive approach to simultaneously solve the energy crisis and global warming problem. Herein, comparative photocatalytic activity of graphene oxide nanosheets have been investigated for photocatalytic reduction of CO_2 into methane and methanol in continuous gas and liquid phase photoreactor system. The graphene oxide sheets were prepared according to Tour's method. The chemical composition and optical properties was evaluated through XPS and UV-vis spectroscopy. Graphene oxide nanosheets exhibited maximum amount of 224.87 μmol/g.h methanol and 14.8 μmol/g.h methane in liquid and gas phase system, respectively. Higher yield of methanol in liquid phase compared to methane in gaseous system can be attributed to dispersion of graphene oxide sheets in water. Hence, graphene oxide nanosheets are efficient photocatalyst for CO_2 reduction into methanol. Nevertheless, further research is essential to improve the photostability of graphene oxide sheets for real application of photocatalytic CO_2 reduction.

Keywords: Carbon dioxide; graphene oxide; methane; methanol.

INTRODUCTION

Energy requirement of the world is increasing day by day due to growing population and advancements in scientific inventions. Fossil fuels are considered as primary source of energy and combustion of fossil fuel is polluting the environment particularly the global warming due to uncontrolled emission of carbon dioxide (CO_2). Reduction of CO_2 is essential to curb the global warming and save the environment [1-3]. Several processes have been used to reduce the level of CO_2 such as carbon capture and storage, conventional absorption, biological, chemical and thermochemical reduction of CO_2 [4-8]. Although, all processes are under development stages, they suffer from the higher cost and environmental limitations. Photocatalytic reduction of CO_2 is the most economical and environmental friendly process using renewable sunlight energy [9-12].

Photocatalytic reduction of CO_2 was pioneered by Inoue and Fujishima in 1979 [13]. Environmental friendly photocatalyst with novel properties that can enhance the

process efficiency, have been the interest of researchers. Several semiconductors such as zirconium oxide [14], gallium oxide [15], magnesium oxide [16], zinc sulfides [17], cadmium sulfides [18], bismuth sulfide [19], graphitic carbon nitride [20] and titanium oxide (TiO_2) [21] have been employed as photocatalyst. Among all, TiO_2 has been the widely reported photocatalyst because of its unique properties, high stability, availability and non-toxicity [22-25]. However, photocatalytic activity of TiO_2 is limited due to large bandgap energy and electrons-holes recombination problem. Lot of efforts have been made to improve the activity of TiO_2 via coupling/doping with metals and non-metals [26, 27]. However, photocatalytic efficiency of TiO_2 is far from practical applications.

Graphene is a two dimensional (2D) single layered atomic sheet with hexagonal structures and zero bandgap material [28]. Meanwhile, GO which is oxygenated graphene sheets, comprise of covalently and non-covalently bonded oxygen functional groups such as epoxy, phenolic and carboxylic group [29]. In past few years, graphene based photocatalytic semiconductors have widely reported for CO_2 reduction due to their excellent activity [30]. Distinguish feature of graphene base materials is fast transportation of charge carriers and lower charge recombination across photocatalyst [31, 32]. The GO has wide bandgap energy and great potential to act as photocatalyst for CO_2 reduction into useful product such as methane, methanol and formic acid.

Generally, GO has been synthesized by Brodie [33], Staudenmaier [34] and hummer's method [35]. Pros and cons of different methods has been enlisted by Lavin-Lopez et al. [36]. Most commonly used hummer's method involves oxidation of graphite using strong oxidizing agent such as H_2SO_4, $KMnO_4$ and $NaNO_3$ respectively. Incomplete oxidation and release of toxic gas are drawbacks of hummer's method. Recently, Tour et al. [37] have developed the safest approach as compared to hummer's method by replacing $NaNO_3$ by H_3PO_4.

In the present study, GO was synthesized according to Tour's method as it gives higher yield and minimal basal defects in GO. According to our knowledge, there is limited study on direct use of GO in photocatalytic applications. Herein, comparative photocatalytic activity of GO has been investigated for liquid and gas phase CO_2 reduction system.

MATERIALS AND METHOD

Materials

Graphite flakes (< 45 µm, Sigma Aldrich), potassium permanganate, $KMnO_4$ (≥ 99 %, Sigma Aldrich), sulfuric acid, H_2SO_4 (95-98 %, R&M chemicals), phosphoric acid, H_3PO_4 (85 %, R&M chemicals), hydrochloric acid, HCl (37 %, R&M chemicals), hydrogen peroxide, H_2O_2 (30%, Merck), and ethanol absolute, C_2H_5OH (99.99 %, Merck). All chemicals were analytical grade and used as received. Deionized water was used throughout the experiments.

Method

The GO was synthesized according to Tour's method [37] with modified parameters. In simple, 3 g of graphite powder was slowly added to 400 ml of mixed acid (H_2SO_4/H_3PO_4:9/1) in an ice bath to maintain the temperature at 10 °C along with mechanically stirring at 300 rpm. In addition, 18 g of $KMnO_4$ was added slowly and

mixture was shifted into oil bath at the temperature of 50 ^oC and stirred for 24 h. Then, 400 mL (Deionized water) ice was gradually poured into mixture at room temperature followed by dropwise addition of 5 mL of H_2O_2. The color of mixture was turned to yellow indicating the complete oxidation of graphite to graphite oxide. The obtained suspension was then pass through polyester fiber and further centrifuged. Graphite oxide was washed with 10 % HCl (1 litre) and absolute ethanol (500 ml) followed by washing with deionized water. Washing with deionized water continued until pH became neutral (7). Then, recovered graphite oxide was oven-dried at 35 ^oC for two days followed by grinding. Dried graphite oxide was again dispersed into deionized water and sonicated for 1 h to exfoliate it to GO sheets and centrifuged at 1000 rpm (20 min) to remove unoxidized graphite particles. The GO sheets were separated from suspension at high centrifugation speed of 4000 rpm (for 4 h) followed by drying at 35 ^oC.

Characterization

X-ray photoelectron spectroscopy was performed to investigate the surface chemical composition. It was equipped with Al K-α radiations with corrected calibration binding energies against the C1 of carbon fixed at 284.6 eV. XPS spectra was recorded on pass energy of 50-200 eV. UV-visible spectroscopy was used to measure the absorption profile of synthesized photocatalyst. The spectrum measurements were performed using Agilent Cary technologies 100 UV-vis spectrometer Model G9821A with wavelength range of 200-800 nm. The band gap energies of the photocatalyst was measured from the Kubelka–Munk (KM) function.

Photocatalytic Reduction of CO_2

Photocatalytic reduction of CO_2 was carried out in liquid and gas phase continuous flow photoreactor. The gas phase photoreactor was comprise of cylindrical stainless-steel chamber with quartz window on top and 500 W Xenon (Xe) lamp as source of light. Typically, 0.1 g of photocatalyst was uniformly dispersed in photoreactor. Helium (He) gas was passed through reactor for certain time to purge the gaseous impurities from system. Then, CO_2 was bubbled through water bubbler to have mixture of CO_2 and H_2O vapours and passed through reactor for half hour to establish equilibrium in system. Photoreactor was fully covered with aluminium foil to avoid the interference of light from surrounding. The CO_2 flowrate was set at 20 mL/min and lamp was switched on to start the photoreaction. Product was analysed through online GC-TCD&FID. Moreover, FID was coupled with a HP-PLOT Q capillary column (Agilent, length 30 m, ID 0.53 mm, film 40 µm) for the segregation of C1-C6 paraffin and olefin hydrocarbon, alcohols and other oxygenated compounds. TCD was attached to UCW982, DC-200, Porapak Q and Mol Sieve 13X columns. In addition, liquid phase photoreactor was comprising of quartz glass vessel with 500W Xe lamp as source of light. Typically, 0.1 g of photocatalyst was suspended in 100 mL H_2O with continuous stirring. The sodium hydroxide (NaOH) was added into 100 mL H_2O to ensure the higher absorption of CO_2. Prior to start, system was purged with CO_2 for half hour and then CO_2 flow rate was adjusted to 20 mL/min. System was fully covered with aluminium foil to stop the interference of light from surrounding. Lamp was switched on after 30 min so that system should be at steady state and equilibrium condition. Samples were collected after every 30 min and analysed through GC-FID to measure quantity of photoproduct.

RESULTS AND DISCUSSION

XPS Analysis

XPS analysis indicated the chemical structure of prepared GO and nature of surface moieties. Figure 1(a) and (b) show the XPS spectrum of C1s and O1s along with deconvoluted peaks. In XPS spectra of C1s, there are four deconvoluted peaks at 284.28, 285.48, 287.48 and 289.48 eV reflecting the bonding of carbon and oxygen corresponding to C=C, C-O, C=O and -COOH groups. Peak at 284.28 is attributed to C=C bond which represent the sp^2 character of graphene structure. Other peaks can be assigned to C-O (285.48 eV), C=O (287.48 eV) and -COOH (289.48). Furthermore, C-O bond represent the C-O-C (epoxy) bonding and C-OH (phenolic) functional groups attached to the basal planes of graphene sheets [38-40]. In O1s spectra, major peak at 533.48 eV is attributed to aromatic group (C-O) [41]. Percentage area of peak for C=O (287.48 eV) is 38.17 % of total C1s spectra which indicates that most of GO sheets are crowded with carbonyl groups. In addition, O1s spectra exhibited higher percentage of phenolic groups, C-O (40.36 %), at 533.48 eV. Peaks of oxygen functional group along with carbon indicate the oxidation of graphite into GO and would enhance adsorption and photocatalytic reduction of CO$_2$ [42].
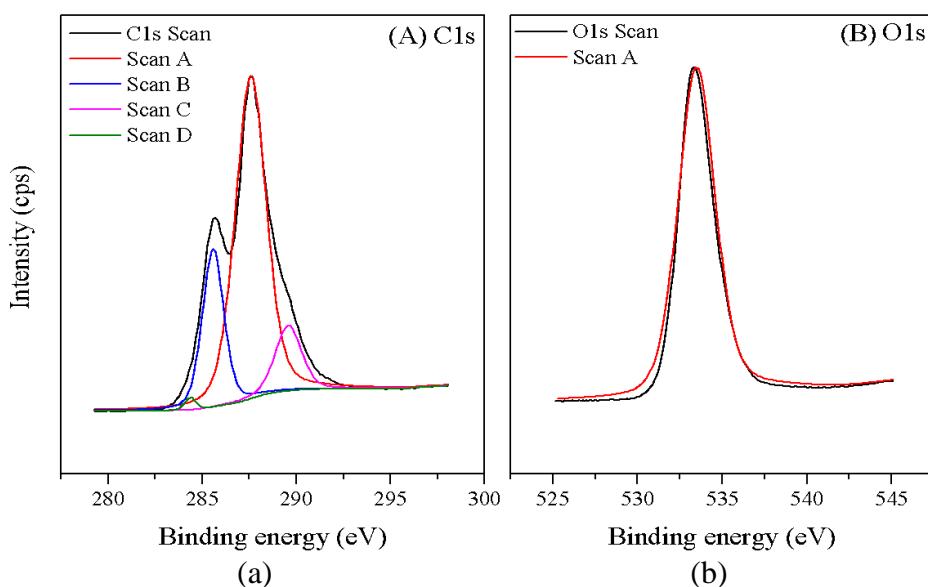

Figure 1. XPS spectrum of (a) C1s (A) and (b) O1s (B).

UV-vis Spectroscopy

Optical response of GO was evaluated through *UV-vis* spectrometer as shown in Figure 2(a). GO exhibited strong light absorption spectra in visible light region and light absorption start to decrease at wavelength (λ) < 400 nm. Higher absorption of visible light compared to *UV* light indicate that GO is more active under visible light irradiations. Response of GO in λ > 400 nm can be attributed to n→π* transition of C=O [29]. Optical band gap of GO calculated by Kubelka-Munk function using Tauc plot was 1.3 eV as shown in Figure 2(b). Bandgap energy of GO depends on oxygen function groups density

and high oxygen density will generate larger bandgap [43]. Low bandgap of 1.3 eV suggest that GO should produce high yield of solar fuel. Huang et al. reported that bandgap energy of GO can be tuned from 2.7 to 1.15 eV depending on density of oxygen functional groups [44]. Thus, Low bandgap energy GO could be efficient photocatalyst for CO_2 reduction to solar fuel under visible light irradiation.
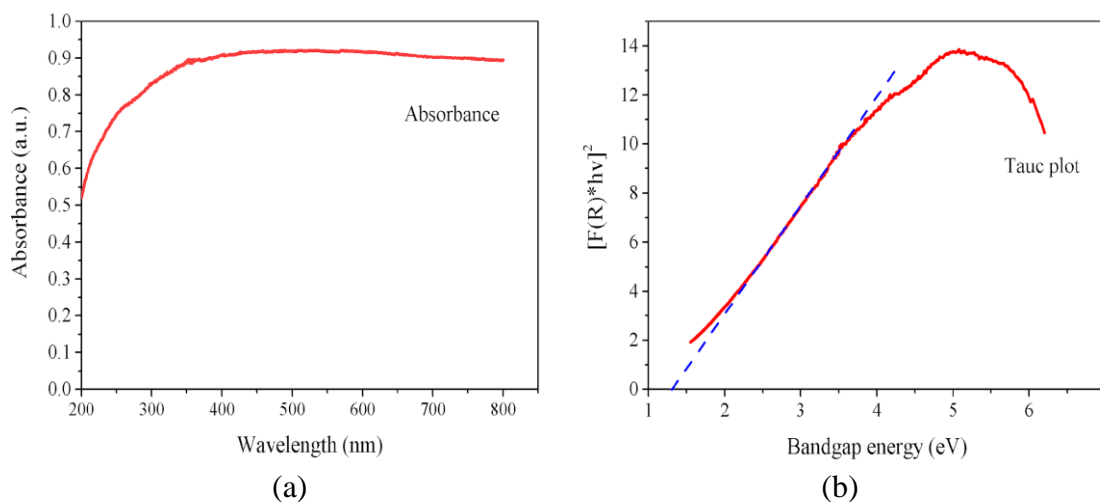

Figure 2. *UV-vis* spectrum (a) and Tauc plot for GO (b)

Photocatalytic Activity

To investigate the photocatalytic performance of GO, CO_2 reduction experiments were carried out in continuous liquid and gas phase photoreactors. Figure 3(a) and (b) show the yield of solar fuels produced in gas and liquid phase, respectively. In gas phase system, CH_4 was detected as main product with maximum yield of 14.8 µmol/g.h. Initially, yield of CH_4 increased till 90 min and then started to decrease. It could be due to instability of photocatalyst caused by accumulation of holes on the surface of GO [30]. In addition, there was no CO in our system, which indicate that GO photocatalyst promote the conversion of CO_2 into CH_4. Formation of CH_4 needs 8 electrons which required high surface electron density and GO exhibited the multielectron reduction process [45]. Quantity of methane was higher as compared to reported value by Tan et al. [46]. Although, significant amount of CH_4 was produced by GO, it suffered from photo stability problem as activity decreased with time [30].

In liquid phase photocatalytic CO_2 reduction, CH_3OH was detected as main product. Significantly, large quantity of 224.87 µmol/g.h of CH_3OH was observed at 60 min but yield decreased sharply with time like gas phase system. According to literature, most of graphene base photocatalyst exhibited the higher production of CH_3OH in liquid phase and CH_4 in gas phase CO_2 reduction system [30]. Decrease in activity of GO in both liquid and gas phase system reflects the photostability problem of material [47]. However, activity was almost similar and constant for 90 min and 120 min which indicate that GO sustained the activity with little decrease of yield in liquid phase system. Most of graphene base photocatalyst produced CH_4 and CH_3OH in gas phase and liquid phase photocatalytic CO_2 reduction [48]. Production of CH_4 and CH_3OH suggest that reduction took place through multielectrons reduction path rather single electron reduction path.

Higher yield of CH_3OH could be attributed to efficient dispersion of GO in water. Moreover, conduction band potential of GO is -0.79 V (*vs*. Normal Hydrogen Electrode (NHE)) which is more negative than reduction potential of CO_2/CH_4 (-0.24 V) and CO_2/CH_3OH (-0.38 V), respectively. Valence band potential of GO is 4 V (*vs*. NHE) which is higher than oxidation potential of H_2O/O_2, H^+ (-0.82) [29]. Although, GO can be potential photocatalyst for the CO_2 reduction into CH_4 and CH_3OH, stability of photocatalyst is to be improved.

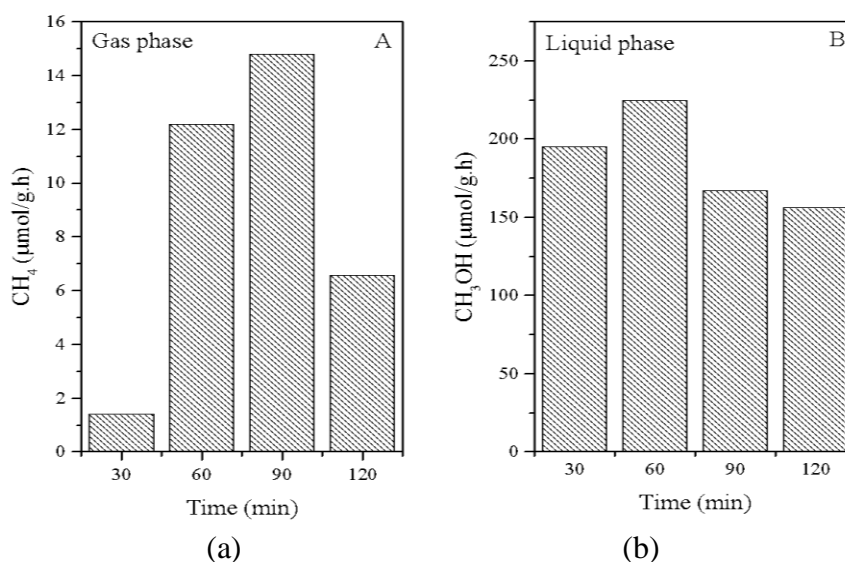
(a)   (b)

Figure 3. Photocatalytic reduction of CO_2 in gas phase (a) and liquid phase (b)

CONCLUSION

GO nanosheets were successfully synthesized according to Tour's method through acid oxidation of graphite flakes. Photocatalytic activity of GO nanosheets was evaluated for the reduction of CO_2 into CH_4 and CH_3OH using gas and liquid phase photoreactor system, respectively. Activity of GO nanosheets was higher in liquid phase system with maximum production 224.87 µmol/g.h of CH_3OH compared to 14.8 µmol/g.h of CH_4 in gas phase system. However, GO sheets were instable due to oxygen groups, and their activity decreased with time in both liquid and gas phase CO_2 reduction system. Further study need to be conducted to improve the photostability and photoactivity of GO nanosheets.

ACKNOWLEDGEMENT

REFERENCES

[1]   Matthews HD, Zickfeld K, Knutti R, Allen MR. Focus on cumulative emissions, global carbon budgets and the implications for climate mitigation targets. Environmental Research Letters. 2018;13:010201.

[2]   Feroskhan M, Ismail S. A review on the purification and use of biogas in compression ignition engines. International Journal of Automotive and Mechanical Engineering. 2017;14;4383-00.

[3]   Pattanaik BP, Jena J, Misra RD. The effect of oxygen content in soapnut biodiesel-diesel blends on performance of a diesel engine. International Journal of Automotive and Mechanical Engineering. 2017;14:4574-88.

[4]   He Q, Yu G, Yan S, Dumée LF, Zhang Y, Strezov V, Zhao S. Renewable CO_2 absorbent for carbon capture and biogas upgrading by membrane contactor. Separation and Purification Technology. 2018;194:207-15.

[5]   Zhang Z, Cai J, Chen F, Li H, Zhang W, Qi W. Progress in enhancement of CO_2 absorption by nanofluids: A mini review of mechanisms and current status. Renewable Energy. 2018;118:527-35.

[6]   Kwon H-S, Park S, Lee C-H, Ahn I-S. CO_2 fixation stability by Sulfurovum lithotrophicum $42BKT^T$ depending on pH and ionic strength conditions. Journal of Industrial and Engineering Chemistry. 2018;57:72-76.

[7]   Halder A, Kilianová M, Yang B, Tyo EC, Seifert S, Prucek R, Panáček A, Suchomel P, et al. Highly efficient Cu-decorated iron oxide nanocatalyst for low pressure CO_2 conversion. Applied Catalysis B: Environmental. 2018;225:128-38.

[8]   Maiti D, Hare B, Daza Y, Ramos AE, Kuhn JN, Bhethanabotla VR. Earth Abundant Perovskite Oxides for Low Temperature CO_2 Conversion. Energy & Environmental Science. 2018.

[9]   Bafaqeer A, Tahir M, Amin NAS. Synthesis of hierarchical ZnV_2O_6 nanosheets with enhanced activity and stability for visible light driven CO_2 reduction to solar fuels. Applied Surface Science. 2018;435:953-62.

[10]   Lin X, Gao Y, Jiang M, Zhang Y, Hou Y, Dai W, Wang S, Ding Z. Photocatalytic CO_2 reduction promoted by uniform perovskite hydroxide $CoSn(OH)_6$ nanocubes. Applied Catalysis B: Environmental. 2018;224:1009-16.

[11]   Ran J, Jaroniec M, Qiao SZ. Cocatalysts in Semiconductor-based Photocatalytic CO_2 Reduction: Achievements, Challenges, and Opportunities. Advanced materials. 2018.

[12]   Low J, Qiu S, Xu D, Jiang C, Cheng B. Direct evidence and enhancement of surface plasmon resonance effect on Ag-loaded TiO_2 nanotube arrays for photocatalytic CO_2 reduction. Applied Surface Science. 2018;434:423-32.

[13]   Inoue T, Fujishima A, Konishi S, Honda K. Photoelectrocatalytic reduction of carbon dioxide in aqueous suspensions of semiconductor powders. Nature. 1979;277:637-38.

[14]   Haas T, Krause R, Weber R, Demler M, Schmid G. Technical photosynthesis involving CO_2 electrolysis and fermentation. Nature Catalysis. 2018;1:32-39.

[15]   Khan I, Qurashi A, Berdiyorov G, Iqbal N, Fuji K, Yamani ZH. Single-step strategy for the fabrication of GaON/ZnO nanoarchitectured photoanode their experimental and computational photoelectrochemical water splitting. Nano Energy. 2018;44:23-33.

[16] Kwak BS, Kim KM, Park S-M, Kang M. Synthesis of basalt fiber@$Zn_{1-x}Mg_xO$ core/shell nanostructures for selective photoreduction of CO_2 to CO. Applied Surface Science. 2017;407:109-16.

[17] Suzuki TM, Takayama T, Sato S, Iwase A, Kudo A, Morikawa T. Enhancement of CO_2 reduction activity under visible light irradiation over Zn-based metal sulfides by combination with Ru-complex catalysts. Applied Catalysis B: Environmental. 2018;224:572-78.

[18] Zhang F, Zhuang HQ, Song J, Men YL, Pan YX, Yu SH. Coupling cobalt sulfide nanosheets with cadmium sulfide nanoparticles for highly efficient visible-light-driven photocatalysis. Applied Catalysis B: Environmental. 2018;226:103-10.

[19] Bai Y, Yang P, Wang P, Xie H, Dang H, Ye L. Semimetal bismuth mediated UV–vis-IR driven photo-thermocatalysis of $Bi_4O_5I_2$ for carbon dioxide to chemical energy. Journal of CO_2 Utilization. 2018;23:51-60.

[20] Jiang Z, Wan W, Li H, Yuan S, Zhao H, Wong PK. A Hierarchical Z-Scheme alpha-Fe_2O_3/g-C_3N_4 Hybrid for Enhanced Photocatalytic CO_2 Reduction. Advanced materials. 2018.

[21] Tahir M. Photocatalytic carbon dioxide reduction to fuels in continuous flow monolith photoreactor using montmorillonite dispersed Fe/TiO_2 nanocatalyst. Journal of Cleaner Production. 2018;170:242-50.

[22] Kumar S, Jain S, Yadav Lamba B, Kumar P. Epigrammatic status and perspective of sequestration of carbon dioxide: Role of TiO_2 as photocatalyst. Solar Energy. 2018;159:423-33.

[23] Daud I, Begum S, Rahman M, Gholizadeh S, Kothandapani Z. Investigating the physical and mechanical properties of TiO_2 varistor materials prepared with various dopants. International Journal of Automotive and Mechanical Engineering. 2014;9:1630.

[24] Ali N, Mustapa M, Ghazali M, Sujitno T, Ridha M. Fatigue life prediction of commercially pure titanium after nitrogen ion implantation. International Journal of Automotive and Mechanical Engineering. 2013;7:1005.

[25] Aznilinda Z, Herman S, Ramly M, Raudah A, Rusop M. Memristive behavior of plasma treated TiO_2 thin films. International Journal of Automotive and Mechanical Engineering. 2013;8:1339.

[26] Ambrožová N, Reli M, Šihor M, Kuśtrowski P, Wu JCS, Kočí K. Copper and platinum doped titania for photocatalytic reduction of carbon dioxide. Applied Surface Science. 2018;430:475-87.

[27] Zhang R, Wang L, Kang Z, Li Q, Pan H. Effect of photocatalytic reduction of carbon dioxide by N-Zr co-doped nano TiO_2. Environmental technology. 2017;38:2677-83.

[28] Novoselov KS, Geim AK, Morozov SV, Jiang D, Zhang Y, Dubonos SV, Grigorieva IV, Firsov AA. Electric field effect in atomically thin carbon films. science. 2004;306:666-69.

[29] Hsu HC, Shown I, Wei HY, Chang YC, Du HY, Lin YG, Tseng CA, Wang CH, et al. Graphene oxide as a promising photocatalyst for CO_2 to methanol conversion. Nanoscale. 2013;5:262-68.

[30] Yang MQ, Xu YJ. Photocatalytic conversion of CO_2 over graphene-based composites: current status and future perspective. Nanoscale Horizons. 2016;1:185-200.

[31]   Bafaqeer A, Tahir M, Amin NAS. Synergistic effects of 2D/2D ZnV_2O_6/RGO nanosheets heterojunction for stable and high-performance photo-induced CO_2 reduction to solar fuels. Chemical Engineering Journal. 2018;334:2142-53.

[32]   Lang Q, Chen Y, Huang T, Yang L, Zhong S, Wu L, Chen J, Bai S. Graphene "bridge" in transferring hot electrons from plasmonic Ag nanocubes to TiO_2 nanosheets for enhanced visible light photocatalytic hydrogen evolution. Applied Catalysis B: Environmental. 2018;220:182-90.

[33]   Brodie B.C. XXIII.—Researches on the atomic weight of graphite. Quarterly Journal of the Chemical Society of London. 1860;12:261-68.

[34]   Staudenmaier L. Verfahren zur darstellung der graphitsäure. European Journal of Inorganic Chemistry. 1899;32:1394-99.

[35]   Hummers Jr WS, Offeman RE. Preparation of graphitic oxide. Journal of the American Chemical Society. 1958;80:1339-39.

[36]   Lavin-Lopez MdP, Romero A, Garrido J, Sanchez-Silva L, Valverde JL. Influence of Different Improved Hummers Method Modifications on the Characteristics of Graphite Oxide in Order to Make a More Easily Scalable Method. Industrial & Engineering Chemistry Research. 2016;55:12836-47.

[37]   Marcano DC, Kosynkin DV, Berlin JM, Sinitskii A, Sun Z, Slesarev A, Alemany LB, Lu W, et al. Improved synthesis of graphene oxide. 2010.

[38]   Liu N, Huang W, Zhang X, Tang L, Wang L, Wang Y, Wu M. Ultrathin graphene oxide encapsulated in uniform MIL-88A(Fe) for enhanced visible light-driven photodegradation of RhB. Applied Catalysis B: Environmental. 2018;221:119-28.

[39]   Lv X, Yang Y, Tao Y, Jiang Y, Chen B, Zhu X, Cai Z, Li B. A mechanism study on toxicity of graphene oxide to Daphnia magna : Direct link between bioaccumulation and oxidative stress. Environmental Pollution. 2018;234:953-59.

[40]   Wei Y, Jang CH. Liquid crystal as sensing platforms for determining the effect of graphene oxide-based materials on phospholipid membranes and monitoring antibacterial activity. Sensors and Actuators B: Chemical. 2018;254:72-80.

[41]   Sitko R, Turek E, Zawisza B, Malicka E, Talik E, Heimann J, Gagor A, Feist B, et al. Adsorption of divalent metal ions from aqueous solutions using graphene oxide. Dalton Transactions. 2013;42:5682-89.

[42]   Song J, Wang X, Chang C-T. Preparation and characterization of graphene oxide. Journal of Nanomaterials. 2014;2014.

[43]   Velasco-Soto M, Pérez-García S, Alvarez-Quintana J, Cao Y, Nyborg L, Licea-Jiménez L. Selective band gap manipulation of graphene oxide by its reduction with mild reagents. Carbon. 2015;93:967-73.

[44]   Huang H, Li Z, She J, Wang W. Oxygen density dependent band gap of reduced graphene oxide. Journal of Applied Physics. 2012;111:054317.

[45]   Ong WJ, Tan LL, Chai SP, Yong ST, Mohamed AR. Self-assembly of nitrogen-doped TiO_2 with exposed {001} facets on a graphene scaffold as photo-active hybrid nanostructures for reduction of carbon dioxide to methane. Nano Research. 2014;7:1528-47.

[46]   Tan LL, Ong WJ, Chai SP, Mohamed AR. Reduced graphene oxide-TiO_2 nanocomposite as a promising visible-light-active photocatalyst for the conversion of carbon dioxide. Nanoscale research letters. 2013;8:465.

[47]   Lin LY, Nie Y, Kavadiya S, Soundappan T, Biswas P. N-doped reduced graphene oxide promoted nano TiO_2 as a bifunctional adsorbent/photocatalyst for CO_2

photoreduction: Effect of N species. Chemical Engineering Journal. 2017;316:449-60.

[48]   Liang YT, Vijayan BK, Lyandres O, Gray KA, Hersam MC. Effect of dimensionality on the photocatalytic behavior of carbon–titania nanosheet composites: charge transfer at nanomaterial interfaces. The journal of physical chemistry letters. 2012;3:1760-65.